

See discussions, stats, and author profiles for this publication at: <https://www.researchgate.net/publication/264462177>

Structural Elucidation of Sorghum Lignins from an Integrated Biorefinery Process Based on Hydrothermal and Alkaline Treatments

ARTICLE in JOURNAL OF AGRICULTURAL AND FOOD CHEMISTRY · AUGUST 2014

Impact Factor: 2.91 · DOI: 10.1021/jf501669r · Source: PubMed

CITATIONS

7

READS

45

4 AUTHORS, INCLUDING:



Shao-Long Sun

Beijing Forestry University

25 PUBLICATIONS 254 CITATIONS

[SEE PROFILE](#)



Jia-Long Wen

Beijing Forestry University

59 PUBLICATIONS 501 CITATIONS

[SEE PROFILE](#)



Ming-Guo Ma

Beijing Forestry University

86 PUBLICATIONS 1,397 CITATIONS

[SEE PROFILE](#)

Structural Elucidation of Sorghum Lignins from an Integrated Biorefinery Process Based on Hydrothermal and Alkaline Treatments

Shao-Long Sun,[†] Jia-Long Wen,[†] Ming-Guo Ma,[†] and Run-Cang Sun^{*,†,‡}

[†] Beijing Key Laboratory of Lignocellulosic Chemistry, Beijing Forestry University, Beijing 100083, China

[‡] State Key Laboratory of Pulp and Paper Engineering, South China University of Technology, Guangzhou 510640, China

ABSTRACT: An integrated process based on hydrothermal pretreatment (HTP) (i.e., 110–230 °C, 0.5–2.0 h) and alkaline post-treatment (2% NaOH at 90 °C for 2.0 h) has been performed for the production of xylooligosaccharide, lignin, and digestible substrate from sweet sorghum stems. The yield, purity, dissociation mechanisms, structural features, and structural transformations of alkali lignins obtained from the integrated process were investigated. It was found that the HTP process facilitated the subsequent alkaline delignification, releasing lignin with the highest yield (79.3%) and purity from the HTP residue obtained at 190 °C for 0.5 h. All of the results indicated that the cleavage of the β -O-4 linkages and degradation of β - β and β -5 linkages occurred under the harsh HTP conditions. Depolymerization and condensation reactions simultaneously occurred at higher temperatures (\geq 170 °C). Moreover, the thermostability of lignin was positively related to its molecular weight, but was also affected by the inherent structures, such as β -O-4 linkages and condensed units. These findings will enhance the understanding of structural transformations of the lignins during the integrated process and maximize the potential utilizations of the lignins in a current biorefinery process.

KEYWORDS: sweet sorghum stem, hydrothermal pretreatment, alkaline treatment, lignin, structural feature, nuclear magnetic resonance (NMR)

INTRODUCTION

The ultimate goal of lignocellulosic biomass separation according to the biorefinery was to attain the fractionation of the three primary components (cellulose, hemicelluloses, and lignin) via an effective method, in which the fractions obtained can be converted into different biobased products. Currently, most research has focused on the applications of cellulose in biomass, such as papermaking and cellulosic ethanol production. However, research and development activities directed toward commercial production of cellulosic ethanol have created the opportunity to dramatically increase the transformation of lignin to value-added products.¹ Meanwhile, to maximize the utilization of underlying values of lignocelluloses, it is very important to fractionate them into their main compositions and then transform them into value-added products.²

To investigate the utilization of potential values of lignocelluloses, a series of lignocellulosic biorefinery technologies including steam explosion, extrusion process, dilute acid, and hydrothermal treatment have been investigated.^{3–6} Among them, hydrothermal pretreatment, a process that disposes of lignocelluloses in a chemical-free, water-only medium, provides a low-cost, handy, and environmentally friendly biorefinery technology.⁶ Moreover, physical changes induced by hydrothermal pretreatment that improve enzymatic hydrolysis of cellulose are well-known and include an increase in pore size to enhance enzyme penetration and an increase in accessible cellulose by decreasing its crystallinity and association with lignin.^{7,8} Simultaneously, a hydrothermal pretreatment process can produce some chemicals, such as oligosaccharides, furfural, formic acid, acetic acid, and levulinic acid.⁹ More importantly, hydrothermal pretreatment accelerates the subsequent deligni-

fication. For instance, it has been demonstrated that hydrothermal pretreatment facilitated kraft pulping of hardwood and the subsequent alkaline extraction of lignin.¹⁰ Some integrated biorefinery technologies based on liquid hot water and H₂SO₄ catalysis were also proposed.¹¹ These technologies cause structural changes of lignin and cellulose as well as solubilization of hemicellulose, which in turn contribute to the reduction of biomass recalcitrance. However, the delignification in this process was performed under acidic conditions, which normally needs appropriate acid-resistant equipment. This undoubtedly increases the cost of the entire process.

Sweet sorghum is considered a potential renewable source of energy for economic development and environmental sustainability, owing to its wide adaptability and high photosynthesis.¹⁰ On the basis of previous investigations,^{11,12} a combination of hydrothermal pretreatment (i.e., 110–230 °C, 0.5–2.0 h) and sodium hydroxide delignification was proposed in this study. In this integrated process, alkaline treatment has been implemented to disrupt the dense cellular structure in lignocelluloses.¹³ It contains many types of chemical reactions in the complex network of lignocelluloses, such as cleavage of ether linkages in lignin units along with peeling reaction of carbohydrates.¹⁴ As a biorefinery process, lignin should receive wide attention due to its potential value in developing biobased materials and chemicals. Although the lignin polymers formed during the hydrothermal pretreatment process were structurally

Received: April 8, 2014

Revised: July 29, 2014

Accepted: July 29, 2014

Published: July 29, 2014

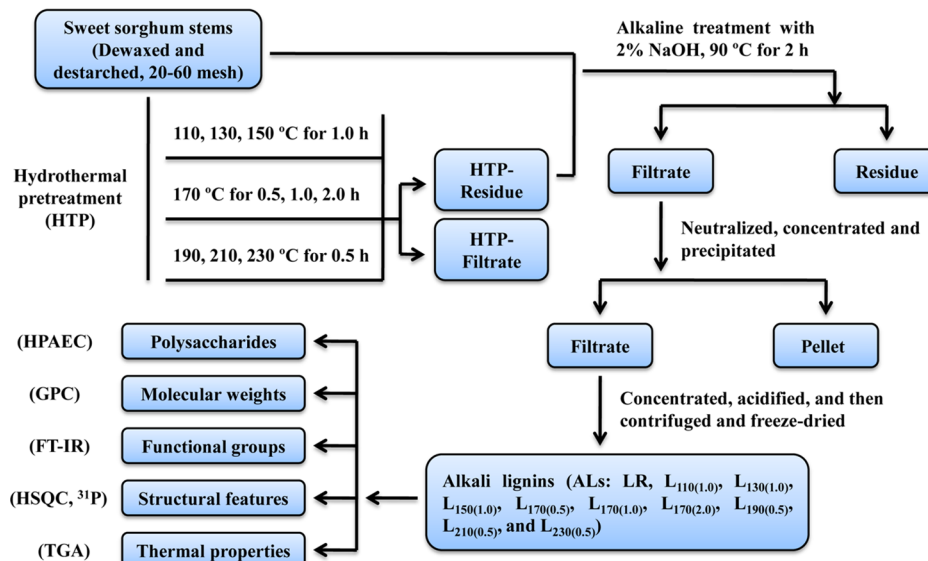


Figure 1. Schematic diagram of the lignin extracted from the integrated process.

analyzed previously, some aspects about lignin yield, purity, dissociation mechanisms, and structural features as well as the structural changes during the integrated process should be clarified in the current integrated process.¹⁵ Moreover, these aspects will be conducive for developing renewability, availability, and value-added lignin-based products, such as sustainable construction materials for replacing petroleum-based products.^{16–18}

In the present study, the structural features and chemical reactivity of the lignin fractions obtained from the integrated process were thoroughly investigated by high-performance anion exchange chromatography (HPAEC), gel permeation chromatography (GPC), and Fourier transform infrared (FT-IR), quantitative two-dimensional heteronuclear single-quantum coherence (2D-HSQC), and ³¹P NMR spectroscopy. In addition, to unveil the relationship between structural features and thermal behaviors, thermogravimetric analysis (TGA) was also performed. It is believed that all of the investigations will increase the availability of these integrated techniques in the current biorefinery industry.

MATERIALS AND METHODS

Materials. Sweet sorghum stems (SSS) were obtained from the experimental farm of the North-Western University of Agricultural and Forest Sciences and Technology (Yangling, People's Republic of China). The dried SSS were cut into small pieces and then ground, and the fractions passing 20–60 mesh were collected. The powder was extracted with toluene/ethanol (2:1, v/v) in a Soxhlet instrument for 6 h, followed by a hot water treatment at 80 °C for 2 h to remove starch. The composition of SSS was 2.3% arabinan, 0.7% galactan, 41.1% glucan, 25.9% xylan, and 21.4% lignin (19.5% Klason lignin and 1.9% acid-soluble lignin), which was determined by using National Renewable Energy Laboratory's (NREL) standard analytical procedure.¹⁹ All experiments were performed in duplicate under the same conditions.

Hydrothermal Pretreatment (HTP). The HTP processes were implemented in a 1000 mL stainless steel autoclave (Parr, USA) with a magnetic stirrer at a solid to liquid ratio of 1:10 (g/mL) by a PID controller (Parr 4848, USA). A total of 15.0 g of raw material was mixed with 150 mL of deionized water and then heated at 110, 130, and 150 °C for 1.0 h, at 170 °C for 0.5, 1.0, and 2.0 h, and at 190, 210, and 230 °C for 0.5 h, respectively. At the end of HTP, the mixtures were cooled to room temperature. The solid residues were collected

with a Buchner funnel, washed thoroughly with distilled water, and further dried in an oven at 60 °C for 16 h.

Alkaline Post-treatment. The unpretreated SSS meal was utilized as starting material for the fractionation process (Figure 1). Specifically, the fractionation (5.0 g HTP residue) was operated in 2% NaOH aqueous solution at 90 °C for 2 h under a solid to liquid ratio of 1:20 (g/mL). The collected liquid fractions were neutralized to pH 5.5–6.0 with 6 M HCl and were further concentrated to 40 mL under vacuum. Subsequently, each concentrated solution was poured into 95% ethanol (120 mL) with vigorous stirring, and the hemicellulosic pellet was obtained by filtering, washing with 70% aqueous ethanol, and freeze-drying. The residual supernatants were concentrated to 30 mL and poured in 150 mL of acidic water (pH 2.0, adjusted by HCl) to precipitate the lignins (i.e., alkali lignins, ALs). The notation of the nine ALs ($L_{110(1.0)}$, $L_{130(1.0)}$, $L_{150(1.0)}$, $L_{170(0.5)}$, $L_{170(1.0)}$, $L_{170(2.0)}$, $L_{190(0.5)}$, $L_{210(0.5)}$, and $L_{230(0.5)}$) was according to the increasing pretreatment conditions (i.e., 110–230 °C, 0.5–2.0 h). Raw lignin (LR) was also separated from the unpretreated SSS under the same alkaline treatment condition.

Analysis Procedures. The associated polysaccharides in the ALs were calculated by using HPAEC as reported previously.²⁰ Molecular weights of the ALs were determined by GPC with an ultraviolet detector (UV) at 240 nm. The column used was a PL-gel 10 mm mixed-B 7.5 mm i.d. column, which was calibrated with PL polystyrene standards. Four milligrams of the ALs was dissolved in 2 mL of tetrahydrofuran (THF), and 20 μL lignin solutions were injected. The column was operated at ambient temperature and eluted with THF at a flow rate of 1.0 mL/min. FT-IR spectra of the ALs were recorded on a Bruker spectrophotometer in the range of 800–2000 cm⁻¹ with a resolution of 4 cm⁻¹. A KBr disk containing 1% finely ground ALs was used for determination. The solution-state NMR spectra of the ALs were acquired on a Bruker AVIII 400 MHz spectrometer at 25 °C. For 2D HSQC spectroscopic experiments, the data were acquired in HSQC experiment mode using 60 mg of lignin in 0.5 mL of DMSO-*d*₆. Functional groups (phenolic hydroxyl, aliphatic hydroxyl, and carboxyl groups) of the ALs were determined by ³¹P NMR spectra according to recent publications.^{21,22} Thermal properties of the ALs were measured by using TGA and differential thermogravimetric (DTG) analysis on a simultaneous thermal analyzer (TGA Q500, USA). About 4–8 mg of the AL samples was heated in a platinum crucible from room temperature to 700 °C at a heating rate of 20 °C/min under nitrogen atmosphere. Provision was made for electronic differentiation of the weight signal to give the rate of weight loss.²⁰

Table 1. Solid Yields, Yields, and Contents of Associated Polysaccharides of the Alkali Lignins Obtained from the Integrated Process under Various Processing Conditions

temperature (°C)–time (h)	solid yield (%)	lignin fraction	total sugars ^a	arabinose	galactose	glucose	xylose	yield ^b
control	100	LR ^c	2.9	0.7	0.3	0.3	1.6	30.7
110–1.0	92.4	L _{110(1.0)}	1.3	0.3	ND ^d	0.2	0.8	52.3
130–1.0	88.1	L _{130(1.0)}	1.8	0.3	0.2	0.2	1.1	53.4
150–1.0	77.3	L _{150(1.0)}	1.4	0.4	ND	0.2	1.2	54.9
170–0.5	68.6	L _{170(0.5)}	1.7	0.1	ND	0.2	1.4	59.6
170–1.0	64.6	L _{170(1.0)}	1.2	ND	ND	0.1	1.1	64.7
170–2.0	61.9	L _{170(2.0)}	0.8	ND	ND	0.1	0.7	61.6
190–0.5	60.3	L _{190(0.5)}	1.2	ND	ND	0.1	1.1	79.3
210–0.5	58.5	L _{210(0.5)}	ND	ND	ND	ND	ND	54.8
230–0.5	51.5	L _{230(0.5)}	ND	ND	ND	ND	ND	39.9

^aBased on the dry mass of lignin (% w/w). ^bBased on the Klason lignin content in the corresponding SSS (% w/w). ^cL_{110(1.0)}, L_{130(1.0)}, L_{150(1.0)}, L_{170(0.5)}, L_{170(1.0)}, L_{170(2.0)}, L_{190(0.5)}, L_{210(0.5)}, and L_{230(0.5)} represent the lignin fractions isolated by extraction with 2.0% NaOH aqueous solution at 90 °C for 2 h corresponding to the hydrothermal pretreatment temperature–time at 110 °C–1.0 h, 130 °C–1.0 h, 150 °C–1.0 h, 170 °C–0.5 h, 170 °C–1.0 h, 170 °C–2.0 h, 190 °C–0.5 h, 210 °C–0.5 h, and 230 °C–0.5 h, respectively. LR was also fractionated from the unpretreated SSS under the same alkaline treatment condition. ^dND, not detectable.

Table 2. Weight-Average (M_w) and Number-Average (M_n) Molecular Weights and Polydispersities (M_w/M_n) of the Alkali Lignins Obtained from the Integrated Process under Various Processing Conditions

	LR	L _{110(1.0)}	L _{130(1.0)}	L _{150(1.0)}	L _{170(0.5)}	L _{170(1.0)}	L _{170(2.0)}	L _{190(0.5)}	L _{210(0.5)}	L _{230(0.5)}
M_w	1360	1320	1300	1280	1100	1030	790	720	600	530
M_n	1100	1020	950	880	730	720	570	490	380	340
M_w/M_n	1.24	1.29	1.37	1.45	1.51	1.43	1.39	1.47	1.58	1.56

RESULTS AND DISCUSSION

Solid Yields, Yields, and Associated Polysaccharides of the Lignins. Table 1 shows that the solid yields decreased from 92.4 to 51.5 g/100 g oven-dried SSS as the pretreatment severity increased. This is mainly due to the degradation and solubilization of hemicelluloses. According to the NREL procedure, the Klason lignin contents in respective HTP residues obtained from the different pretreatment conditions (110, 130, 150 °C for 1.0 h; 170 °C for 0.5, 1.0, 2.0 h; and 190, 210, 230 °C for 0.5 h) were 16.5, 19.2, 20.7, 24.1, 24.7, 25.7, 28.0, 33.6, and 43.9%, respectively. The yields of the ALs were calculated on the basis of the Klason lignin in respective SSS and are shown in Table 1. In the integrated process, the yields of the ALs were 52.3, 53.4, 54.9, 59.6, 64.7, 61.6, 79.3, 54.8, and 39.9%, corresponding to the HTP conditions at 110, 130, 150 °C for 1.0 h; 170 °C for 0.5, 1.0, 2.0 h; and 190, 210, 230 °C for 0.5 h, respectively. Particularly, only 30.7% of the alkali lignin (LR) from the unpretreated SSS was obtained. All data indicated that the HTP process facilitated more original lignin (40.9–68.6%) release with alkaline treatment as compared with direct alkaline delignification (30.7%) without the HTP process. In other words, the HTP was a promising pretreatment for efficiently loosening the tight cell wall structure and then facilitating the release of lignin from the plant cell wall with the assist of alkaline treatment. Apparently, the increase of pretreatment temperature from 110 to 170 °C for 1.0 h resulted in a notable increase of the AL yield from 52.3 to 64.7%. The increasing trend was probably related to the HTP process, which cleaved the chemical bonds between lignin and hemicelluloses to some extent (e.g., ester and ether bonds).²³ The partly dissociated components facilitated the following alkaline extraction under the conditions given. However, when the pretreatment temperature was further increased to 230 °C, the yield of the AL distinctly decreased to 39.9%. Meanwhile, when the pretreatment period was further prolonged from 1.0

to 2.0 h at 170 °C, the yields of the ALs decreased from 64.7 to 61.6%. The reduced yield was due to the fact that the lignin content in the HTP residues was overestimated by the Klason method because the HTP process under the harsh conditions induced some recondensation reactions between polysaccharides (or polysaccharide degradation products) and lignin, which was also called “pseudolignin”.²⁴ Interestingly, the yield of the AL reached a plateau (L_{190(0.5)}, 79.3%) at the pretreatment condition of 190 °C for 0.5 h, demonstrating that the optimized condition for isolating lignin was achieved at this HTP condition. To verify the purity of the extracted ALs, the associated polysaccharides of the ALs were detected by HPAEC (Table 1). As can be seen, all of the ALs contained a rather low amount of associated polysaccharides (<1.80%). In detail, xylose was the major monosaccharide in the ALs, suggesting that the associated polysaccharides in the ALs originated from xylans. Especially, polysaccharides were not detected in L_{210(0.5)} and L_{230(0.5)}, suggesting that the hemicellulosic polymer was thoroughly destroyed and degraded under the harsh conditions.

Molecular Weight Determination. Changes in molecular weights of the ALs indirectly provided valuable insights into lignin’s fragmentation and recondensation reactions during the HTP process. To determine the effect of the HTP on the molecular weight of the ALs obtained, the LR and pretreated lignin fractions (L_{110(1.0)}–L_{230(0.5)}) were analyzed by GPC. Table 2 lists the changes in molecular weight of the ALs with respect to the HTP temperature and time. As shown in Table 2, the molecular weight (M_w) of LR was 1360 g mol⁻¹, and its polydispersity (M_w/M_n) was 1.24. After the HTP, it was observed that the M_w of the ALs decreased (530–1320 g mol⁻¹) as compared to LR. This suggested that the ALs underwent depolymerization with increasing HTP temperature and time.^{23,25} It was noted that the depolymerization reaction became more evident under the harsh pretreatment conditions (HTP temperature was higher than 170 °C and/or time exceeded 1.0 h at 170 °C), which resulted in a reduced M_w of

the ALs ($L_{170(2.0)}$, $L_{190(0.5)}$, $L_{210(0.5)}$, and $L_{230(0.5)}$). Furthermore, the content of β -O-4 was positively related to the M_w of the lignin under the conditions given.²⁶ Especially, the higher the β -O-4 content, the higher the molecular weight of the lignin, which was further confirmed by the subsequent quantitative 2D-HSQC results. Moreover, the polydispersity index of LR obtained from the unpretreated material was 1.24. After the HTP under various processing conditions, the polydispersity indices of the ALs were slightly increased (1.29–1.58) to some extent, suggesting that some inhomogeneous lignin fragments, which were probably originated from HTP and alkaline treatments, occurred and collected after the integrated process.

FT-IR Spectral Analysis. Figure 2 exhibits the fingerprint region of FT-IR spectra of the ALs obtained from the

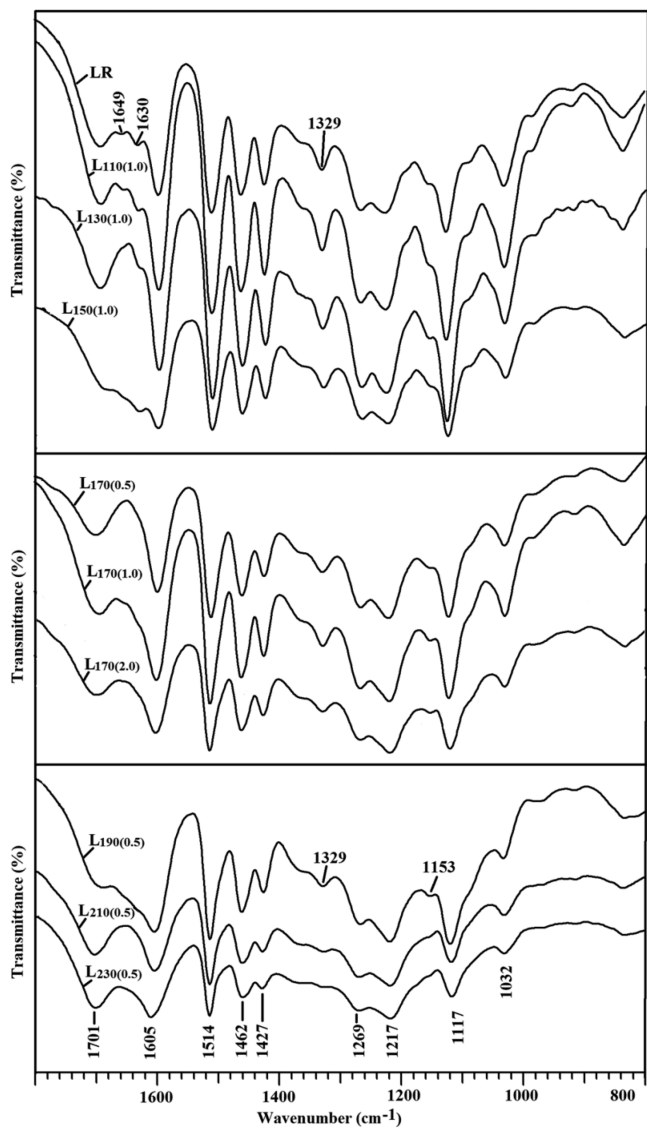


Figure 2. FT-IR spectra of the lignins obtained from the integrated process under various processing conditions.

integrated process, and the bands were assigned according to the literature.^{20,27,28} Specifically, the 1701 cm^{-1} band is attributed to the conjugated/unconjugated carboxyl acid/ester groups or unconjugated β -ketone carbonyl groups. The bands at 1630 – 1649 cm^{-1} originate from stretching of conjugated $\text{C}=\text{O}$ groups, which were prominent in the LR, $L_{110(1.0)}$, and

$L_{130(1.0)}$, suggesting that more conjugated $\text{C}=\text{O}$ appeared at the mild conditions (below $150\text{ }^{\circ}\text{C}$). The intense bands at 1605 , 1514 , and 1427 cm^{-1} correspond to aromatic skeletal vibrations and the C–H deformation combined with aromatic ring vibration at 1462 cm^{-1} . This suggested that the increase of the pretreatment temperature from 110 to $230\text{ }^{\circ}\text{C}$ and/or time from 0.5 to 2.0 h at $170\text{ }^{\circ}\text{C}$ had no evident influence on the basic lignin structure. A small band at 1153 cm^{-1} (antisymmetric C–O stretching of ester groups) was observed in the spectra of the ALs ($LR-L_{190(0.5)}$), implying that some ester bonds remained under the condition given. However, this band was inconspicuous in the ALs ($L_{210(0.5)}$ and $L_{230(0.5)}$), suggesting that the ester bonds in the lignin macromolecules were significantly cleaved when the HTP temperature reached 210 and $230\text{ }^{\circ}\text{C}$. The intensity of bands at 1329 , 1269 , and 1032 cm^{-1} decreased with increasing pretreatment severity, and the bands are assigned to the characteristic of syringyl and condensed guaiacyl units, the ring breathing with C–O stretching in uncondensed guaiacyl units, and aromatic C–H in-plane deformation, respectively. The 1217 cm^{-1} band originates from the C–C, C–O, and $\text{C}=\text{O}$ stretching. In addition, the band at 1117 cm^{-1} , which was ascribed to aromatic C–H in-plane deformation (typical for S units), decreased in $L_{210(0.5)}$ and $L_{230(0.5)}$, suggesting that the proportion of S-type lignin units was decreased as a result of demethoxylation reactions under the harsh pretreatment conditions.^{27,29}

2D-HSQC NMR Spectral Analysis. 2D-HSQC NMR was used to obtain important structural information on the ALs to accelerate the understanding of the fundamental chemistry of the ALs obtained from the integrated process. The 2D-HSQC spectra and main linkages of these ALs are shown in Figures 3 and 4, and the signals were assigned (Table 3) on the basis of previous literature.^{20,21,23,28–38} In the side-chain region of the AL spectra (Figure 3), cross-peaks of different interunit linkages of the ALs were identified, such as β -aryl-ether (β -O-4, A), resolin (β - β , B), phenylcoumaran (β -5, C), α , β -diaryl ethers (E), and *p*-hydroxycinnamyl alcohol end groups (F). As can be seen, the cross-peaks of methoxy groups ($-\text{OCH}_3$, $\delta_{\text{C}}/\delta_{\text{H}}$ 55.7/3.74) and side chains in β -O-4 substructures (A/A') were the main substructures. In the integrated process, the relative content of different linkages was changed. For instance, the content of β -O-4 linkages was decreased, whereas the content of β -5 linkages was increased, suggesting that the β -O-4 linkages were cleaved as a result of the HTP process. In addition, the cleaved β -O-4 linkages were probably recondensed to form β -5 linkages. Furthermore, it was also noted that lignin–carbohydrate complex (LCC), such as benzyl ether (BE) structure, occurred in the ALs at HTP temperature below $210\text{ }^{\circ}\text{C}$, implying that the BE structure was more stable during the integrated delignification process. However, no signal of the BE was detected in the $L_{210(0.5)}$ and $L_{230(0.5)}$, implying that the BE was completely cleaved when the HTP temperature was $>190\text{ }^{\circ}\text{C}$.²⁹

In the aromatic region of 2D-HSQC spectra (Figure 4) of the ALs, the correlated signals of the ALs from syringyl (S/S'), guaiacyl (G/G'), and *p*-hydroxyphenyl (H) units clearly appeared. Specifically, the S and the C_{α} -oxidized S units (S') signals for $C_{2,6}$ – $H_{2,6}$ correlation were observed at $\delta_{\text{C}}/\delta_{\text{H}}$ 104.1/6.72 and 106.2/7.26, respectively. The G units showed various correlations for C_2 – H_2 ($\delta_{\text{C}}/\delta_{\text{H}}$ 110.8/6.99), C_5 – H_5 ($\delta_{\text{C}}/\delta_{\text{H}}$ 114.9/6.71), and C_6 – H_6 ($\delta_{\text{C}}/\delta_{\text{H}}$ 119.1/6.82), respectively. Moreover, the oxidized G units with a C_{α} ketone (G') exhibited

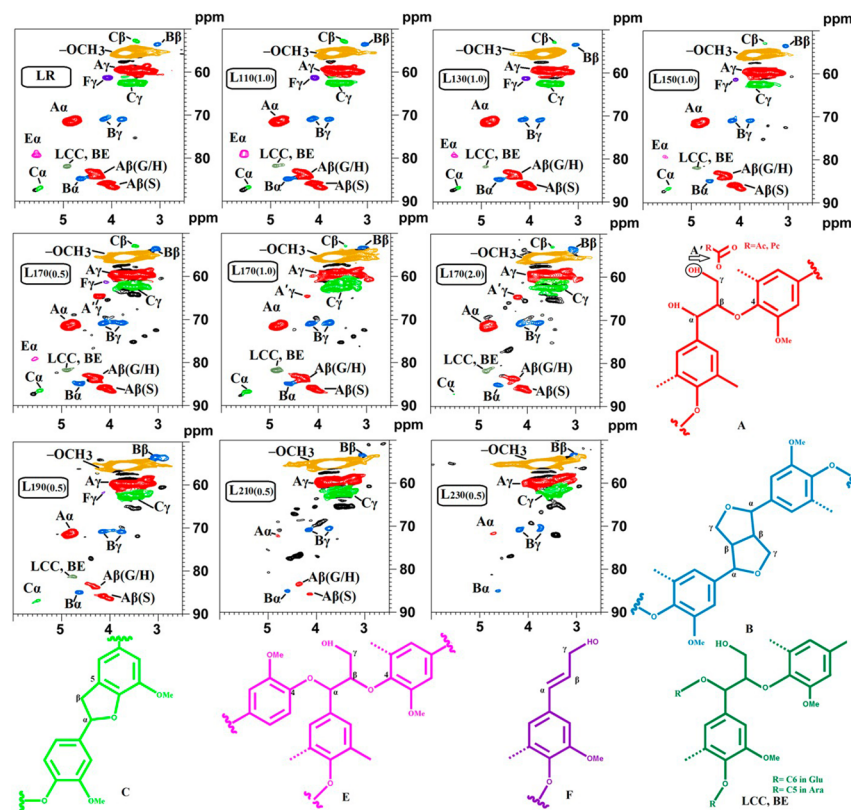


Figure 3. 2D-HSQC spectra and the main structures of the lignins obtained from the integrated process under various processing conditions (side-chain region): (A) β -aryl-ether units (β -O-4); (A') β -O-4 alkyl-aryl ethers with acylated γ -OH with *p*-coumaric acid; (B) resinol substructures (β - β); (C) phenylcoumaran substructures (β -5); (E) α , β -diaryl ethers (α -O-4/ β -O-4). Possible lignin–carbohydrate linkages: (BE) benzyl ether.

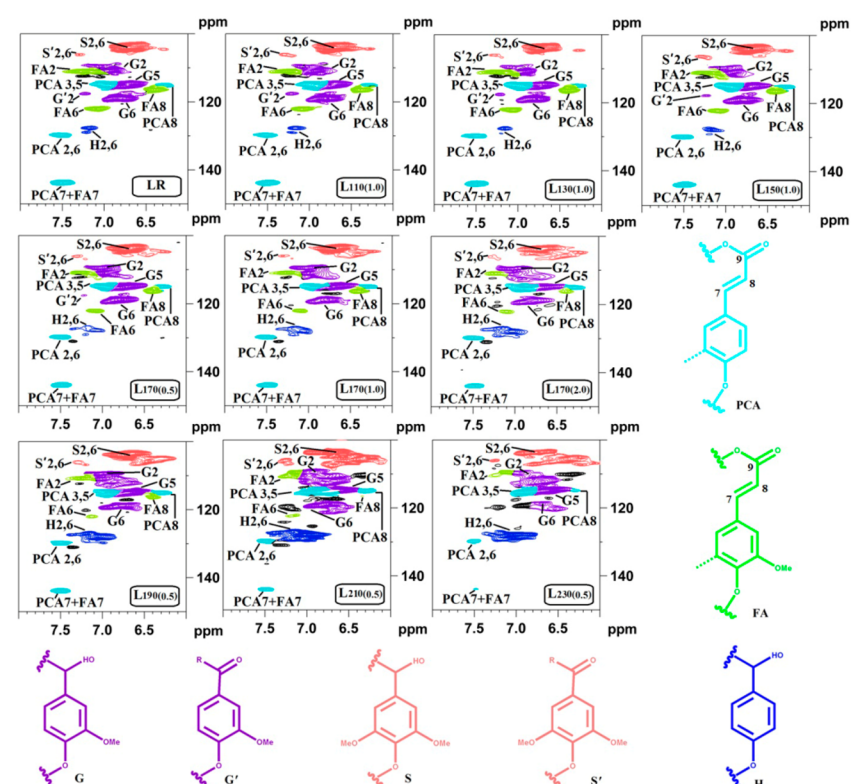


Figure 4. 2D-HSQC spectra and the main structures of the lignin polymers obtained from the integrated process under various processing conditions (aromatic region): (PCA) free *p*-coumaric acid; (FA) ferulate; (H) *p*-hydroxyphenyl units; (G) guaiacyl units; (G') oxidized guaiacyl units with a C_α ketone; (S) syringyl units; (S') oxidized syringyl units bearing a carbonyl at C_α.

Table 3. Assignments of ^{13}C - ^1H Cross-Peaks in HSQC Spectra of the Alkali Lignins from the Integrated Process under Various Processing Conditions

label	$\delta_{\text{C}}/\delta_{\text{H}}$ (ppm)	assignment
C_{β}	52.8/3.48	$\text{C}_{\beta}-\text{H}_{\beta}$ in phenylcoumaran substructures (C)
B_{β}	53.5/3.05	$\text{C}_{\beta}-\text{H}_{\beta}$ in β - β (resinol) substructures (B)
$-\text{OCH}_3$	55.7/3.74	C-H in methoxyls
A_{γ}	59.7/3.62	$\text{C}_{\gamma}-\text{H}_{\gamma}$ in β -O-4 substructures (A)
F_{γ}	61.3/4.09	$\text{C}_{\gamma}-\text{H}_{\gamma}$ in <i>p</i> -hydroxycinnamyl alcohol end groups (F)
C_{γ}	62.4/3.71	$\text{C}_{\gamma}-\text{H}_{\gamma}$ in phenylcoumaran substructures (C)
B_{γ}	71.0/3.79–4.16	$\text{C}_{\gamma}-\text{H}_{\gamma}$ in β - β resinol substructures (B)
$\text{A}_{\alpha(\text{S})}$	71.6/4.83	$\text{C}_{\alpha}-\text{H}_{\alpha}$ in β -O-4 linked to a S unit (A)
E_{α}	78.9/5.55	$\text{C}_{\alpha}-\text{H}_{\alpha}$ in α , β -diaryl ethers (E)
LCC, BE	81.3/4.74	benzyl ether LCC structures
$\text{A}_{\beta(\text{G/H})}$	83.8/4.27	$\text{C}_{\beta}-\text{H}_{\beta}$ in β -O-4 linked to G/H unit (A)
B_{α}	84.8/4.63	$\text{C}_{\alpha}-\text{H}_{\alpha}$ in β - β resinol substructures (B)
$\text{A}_{\beta(\text{S})}$	85.9/4.10	$\text{C}_{\beta}-\text{H}_{\beta}$ in β -O-4 linked to a S unit (A)
C_{α}	87.4/5.56	$\text{C}_{\alpha}-\text{H}_{\alpha}$ in phenylcoumaran substructures (C)
$\text{S}_{2,6}$	104.1/6.72	$\text{C}_{2,6}-\text{H}_{2,6}$ in syringyl units (S)
$\text{S}'_{2,6}$	106.2/7.26	$\text{C}_{2,6}-\text{H}_{2,6}$ in oxidized S units (S')
G_2	110.8/6.99	C_2-H_2 in guaiacyl units (G)
G'_2	117.6/7.22	C_2-H_2 in oxidized G units (G')
G_5	114.9/6.71	C_5-H_5 in guaiacyl units (G)
G_6	119.1/6.82	C_6-H_6 in guaiacyl units (G)
$\text{H}_{2,6}$	127.7/7.17	$\text{C}_{2,6}-\text{H}_{2,6}$ in H units (H)
PCA _{3,5}	115.2/6.92	$\text{C}_{3,5}-\text{H}_{3,5}$ in <i>p</i> -coumaric acid (PCA)
PCA _{2,6}	129.8/7.51	$\text{C}_{2,6}-\text{H}_{2,6}$ in <i>p</i> -coumaric acid (PCA)
PCA ₇	143.9/7.48	C_7-H_7 in <i>p</i> -coumaric acid (PCA)
PCA ₈	115.2/6.29	C_8-H_8 in <i>p</i> -coumaric acid (PCA)
FA ₂	110.9/7.23	C_2-H_2 in ferulic acid (FA)
FA ₆	122.1/7.09	C_6-H_6 in ferulic acid (FA)
FA ₇	143.9/7.48	C_7-H_7 in ferulic acid (FA)
FA ₈	116.5/6.39	C_8-H_8 in ferulic acid (FA)

correlation for C_2-H_2 ($\delta_{\text{C}}/\delta_{\text{H}}$ 117.6/7.22) when the HTP temperature was <170 °C or the HTP time was <1.0 h at 170 °C. However, with further increase of the pretreatment temperature from 170 to 230 °C or increase of the pretreatment time from 1.0 to 2.0 h at 170 °C, no signal of G' was detected in these corresponding ALs, implying the oxidized G units occurred in a relatively low temperature and time. Furthermore, the $\text{C}_{2,6}-\text{H}_{2,6}$ correlation signal from H units was found at $\delta_{\text{C}}/\delta_{\text{H}}$ 127.7/7.17. As the temperature increased, the content of H units increased in the ALs, which was mainly as a result of the demethoxylation reactions occurring in G and/or S units, especially at higher temperatures. Besides the normal signals for aromatic rings of the ALs, some condensed S and G units occurred in the 2D HSQC spectra of the ALs.³⁶ Increasing the pretreatment temperature from 170 to 230 °C or prolonging the pretreatment time from 0.5 to 2.0 h at 170 °C resulted in an obvious increase of the contents of condensed S and G units. The ALs obtained from these processes appeared to contain large amounts of *p*-hydroxycinnamates (PCA and FA). After the same alkaline post-treatment, the lignin obtained (LR-L_{230(0.5)}) presented obvious signals of free *p*-coumaric acid correlations (PCA₈, $\delta_{\text{C}}/\delta_{\text{H}}$ 115.2/6.29) but not for PCA₈ ($\delta_{\text{C}}/\delta_{\text{H}}$ 113.5/6.24), suggesting that the acylated *p*-coumarate (PCE) were significantly cleaved, appeared as free PCA, and coprecipitated

with the alkali lignins, which has been discussed in detail in a previous publication.²⁶ The PCA was characterized by relatively intense correlations at $\delta_{\text{C}}/\delta_{\text{H}}$ 129.8/7.51 (PCA_{2,6}), 115.2/6.92 (PCA_{3,5}), 115.2/6.29 (PCA₈), and 143.9/7.48 (PCA₇), whereas ferulic acid (FA) was found at $\delta_{\text{C}}/\delta_{\text{H}}$ 110.9/7.23 (FA₂), 122.1/7.09 (FA₆), and 116.5/6.39 (FA₈).

Quantitative Analysis of Lignin Structures Based on 2D-HSQC Spectra. The 2D-HSQC spectra of the pretreated lignins illustrated the relative degradation of the lignin side chains and the aromatic units with increasing pretreatment temperature and time as compared to that of the LR. According to the computing method of the literature,^{34,37} the different linkages could be expressed by a comparative mode (Table 4).

Table 4. Quantification of the Alkali Lignins Obtained from the Integrated Process under Various Processing Conditions by Quantitative 2D-HSQC NMR

	β -O-4 ^a	β - β	β -5	α -O-4/ β -O-4	S/G ^b	PCA/FA ^c
LR	54.3	3.2	2.7	3.4	1.16	0.81
L _{110(1.0)}	56.5	7.7	3.4	4.8	1.13	0.71
L _{130(1.0)}	57.5	5.6	3.3	1.8	1.14	1.16
L _{150(1.0)}	47.4	3.6	3.3	1.7	1.36	1.30
L _{170(0.5)}	32.0	5.8	5.7	Tr ^d	1.87	1.78
L _{170(1.0)}	25.6	2.6	3.6	ND ^e	3.13	4.08
L _{170(2.0)}	21.4	3.7	ND	ND	3.76	4.53
L _{190(0.5)}	7.6	1.4	ND	ND	2.87	1.49
L _{210(0.5)}	Tr	Tr	ND	ND	1.81	0.57
L _{230(0.5)}	Tr	Tr	ND	ND	1.19	Tr

^aResults expressed per 100 Ar based on quantitative 2D-HSQC spectra. ^bS/G ratio obtained by the equation S/G ratio = 0.5IS_{2,6}/IG₂.

^cPCA/FA ratio obtained by the equation PCA/FA ratio = 0.5IPCA_{2,6}/IFA₂. ^dTr, trace. ^eND, not detectable.

The content of β -O-4 aryl ether in the ALs obtained at the mild conditions was higher than that of the LR, suggesting that some condensed reactions rather than depolymerization reactions occurred under the mild conditions. The condensation reactions led to the decrease of the protonated aromatic carbon and the elevation the content of β -O-4.²⁹ However, as the pretreatment temperature further increased (150–230 °C), the content of β -O-4 aryl ether in the ALs was sharply decreased, suggesting that the cleavage of β -O-4 aryl ether (depolymerization) was the predominant reaction during the HTP at higher temperatures.

Besides β -O-4 aryl ether linkage cleavage and carbon–carbon linkage degradation or condensation, changes of the S/G and PCA/FA ratios in the ALs were also prominent structural alterations observed after HTP.^{29,38} The S/G and PCA/FA ratios in the ALs had no obvious changes (L_{110(1.0)} and L_{130(1.0)}) at pretreatment temperature <150 °C as compared to that of the LR. The S/G and PCA/FA ratios gradually increased as the pretreatment temperature rose and time prolonged and reached a maximum ratio (S/G = 3.76; PCA/FA = 4.53) in L_{170(2.0)}. The increased S/G ratio suggested that the G-type lignin was more easily degraded during the HTP process, in agreement with a previous study.²⁹ Meanwhile, the increased PCA/FA ratio suggested that most of the etherified FA was removed during the HTP process. However, with the pretreatment temperature further increased from 190 to 230 °C, the S/G and PCA/FA ratios gradually decreased (S/G = 1.19; PCA/FA = 0.94) at the same time in L_{230(0.5)}.

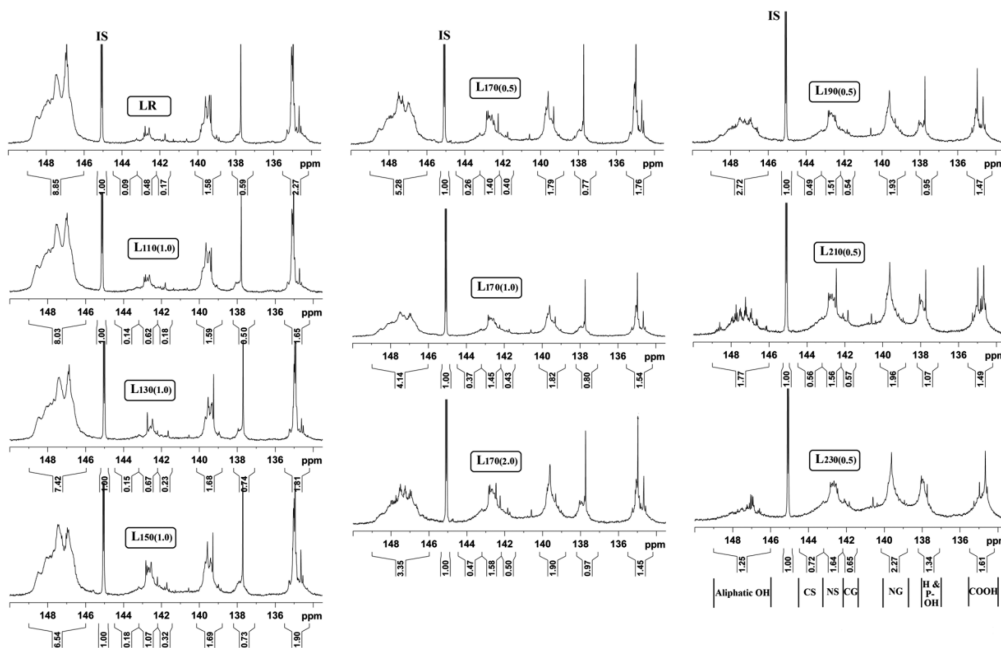


Figure 5. ^{31}P NMR spectra of the lignins obtained from the integrated process under various processing conditions.

Table 5. Quantification of Functional Groups (mmol/g) in Alkali Lignins Obtained from the Integrated Process under Various Processing Conditions by a Quantitative ^{31}P NMR Method^a

lignins	aliphatic OH	syringyl OH		guaiacyl OH		p -hydroxyphenyl OH + PCA-OH	carboxylic group	total phenolic OH
		C	NC	C	NC			
LR	4.79	0.05	0.26	0.09	0.86	0.32	1.23	1.58
L _{110(1.0)}	4.35	0.08	0.34	0.10	0.86	0.27	0.89	1.65
L _{130(1.0)}	4.02	0.08	0.36	0.12	0.92	0.40	0.98	1.88
L _{150(1.0)}	3.54	0.10	0.58	0.17	0.92	0.40	1.03	2.17
L _{170(0.5)}	2.86	0.14	0.76	0.22	0.97	0.42	0.95	2.51
L _{170(1.0)}	2.24	0.20	0.79	0.23	0.99	0.43	0.83	2.64
L _{170(2.0)}	1.81	0.25	0.86	0.27	1.03	0.53	0.79	2.94
L _{190(0.5)}	1.47	0.27	0.82	0.29	1.05	0.51	0.80	2.94
L _{210(0.5)}	0.96	0.30	0.84	0.31	1.06	0.58	0.81	3.09
L _{230(0.5)}	0.68	0.39	0.89	0.35	1.23	0.73	0.87	3.59

^aC, condensed; NC, noncondensed; PCA-OH, free *p*-coumaric acid.

^{31}P NMR Spectral Analysis. To further investigate the fundamental chemistry of the ALs obtained from the integrated process, a quantitative ^{31}P NMR technique was also applied (Figure 5).^{39,40} Table 5 shows the quantitative data on the distribution of the different OH groups of the ALs. The content of aliphatic OH of the ALs gradually reduced as the pretreatment temperature and time increased during the integrated process, suggesting that the aliphatic OH groups were gradually oxidized and modified under the harsh conditions.²⁹ The contents of S- and G-type phenolic OH groups were greatly increased from LR to L_{230(0.5)} as a result of the cleavage of the β -O-4 aryl ether linkages, and the increasing rate of S-type lignin was faster than that of the corresponding G units. Additionally, the gradually increased condensed S and G phenolic OH implied that increasing the pretreatment temperature and time also resulted in more condensation reactions during the HTP process, as shown in the 2D HSQC NMR section aforementioned. The total content of PCA and *p*-hydroxyphenyl OH (H-type lignin unit) could be also revealed by ^{31}P NMR spectra. The total content in LR was 0.32 mmol/g, whereas it decreased to 0.27 mmol/g in L_{110(1.0)} and it increased

from 0.32 to 0.73 mmol/g in the ALs (L_{130(1.0)}–L_{230(0.5)}) as the pretreatment temperature increased from 130 to 230 °C, suggesting that the demethoxylation reactions probably occurred at G and/or S units, especially at higher temperatures, as revealed by the intensive signals of H units in the 2D HSQC spectra.

Thermal Analysis. The thermal behaviors of lignin are extremely important for its utilization in thermochemical conversion into energy and chemicals, for example, thermolysis. The decomposition of lignin is a complex reaction and occurred by diverse bond fissions within the lignin macromolecule. The maximum decomposition temperature (T_M) is the corresponding temperature of the maximum decomposition rate (V_M).⁴¹ In principle, the different thermal behaviors are not only influenced by the inherent structures and different functional groups of lignin molecule but condensation of the lignin macromolecule also associated with specific chemical features. To investigate the potential relationship between structural features and thermal behaviors, the TGA of the ALs (A, LR and L_{150(1.0)}; B, L_{170(0.5)} and L_{170(2.0)}; C, L_{190(0.5)} and L_{230(0.5)}) were comparatively investigated in this experiment (Figure 6).

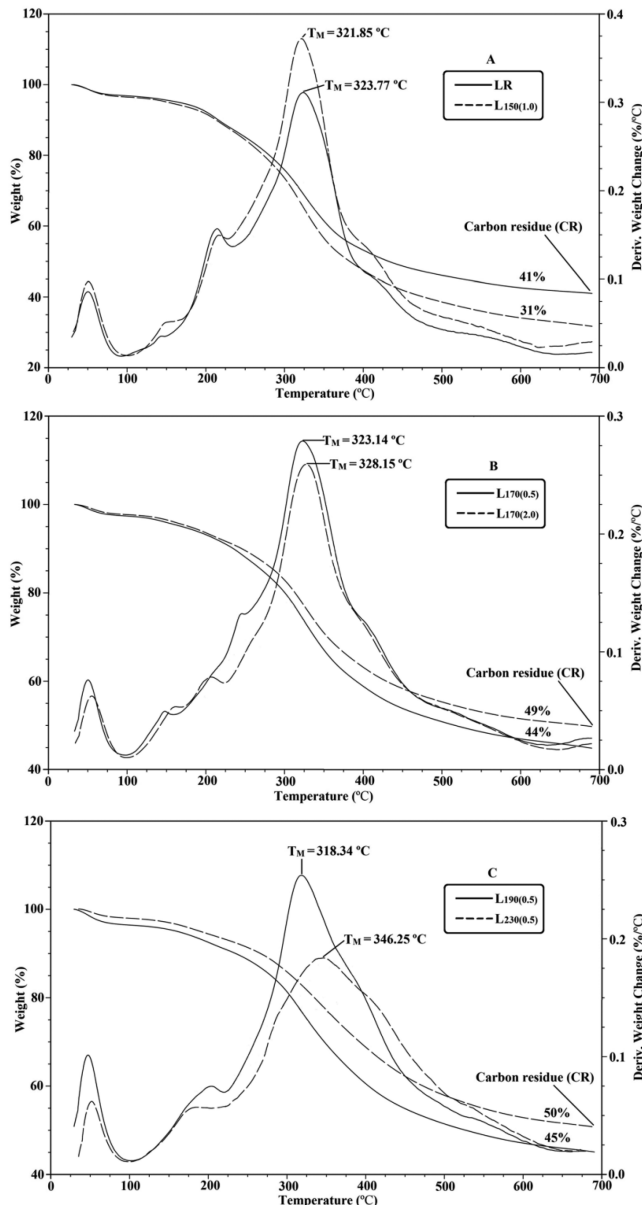


Figure 6. Thermogram of the lignins obtained from the integrated process under various processing conditions.

The T_M of the six ALs obtained from the integrated process existed in the higher T_M range from 318.34 to 346.25 °C. A previous study demonstrated that the T_M is positively correlated with the corresponding molecular weight, suggesting that the initial reaction contained the deformation of the weaker C–O bond in the β -O-4 unit during the lignin decomposition.⁴² In this study, the relationship between T_M and molecular weight reflected only in the ALs extracted from the HTP residue at the mild conditions; however, when the HTP condition became harsh, the lignin extracted contained more condensed units, which in turn affected the corresponding T_M . In addition, “condensed lignin” was also reported to be correlated to “carbon residue (CR).”³⁶ As shown in Figure 6, the CRs were 44% for $L_{170(0.5)}$ and 49% for $L_{170(2.0)}$ at 700 °C as the HTP time increased from 0.5 to 2.0 h at 170 °C (Figure 6B). Similarly, when the HTP temperature further increased from 190 to 230 °C for 0.5 h (Figure 6C), the higher CR was found in $L_{230(0.5)}$ (50%) than in $L_{190(0.5)}$ (45%). That is, the CR

was positively related to the “condensed lignin” of the ALs, which was revealed by the ^{31}P NMR results aforementioned. These facts suggested that lignin with high CR was produced at the harsh HTP conditions.³⁶ However, only a small amount of condensed structures was observed in the ALs at the mild conditions (HTP temperature <170 °C). Therefore, besides the factor of “condensed structures”, the CR in LR was also affected by other factors, such as ash and inorganic salt in plant cell wall.⁴³ This was why the CR in the LR was higher than that of $L_{150(1.0)}$, which even contained a slightly high content of condensed structures.

In summary, the present study demonstrated that the hydrothermally pretreated conditions had significant effects on the subsequent alkali lignin isolation and their chemical structures and properties. It was found that the alkali lignin with a high yield and purity could be obtained from the HTP residue under a high temperature and a short time (190 °C, 0.5 h). Meanwhile, NMR and molecular weight analysis suggested that the cleavage of the β -O-4 linkages and the degradation of β - β and β -5 linkages occurred during the integrated process, especially at the harsh conditions. Depolymerization and condensation reactions mainly occurred at higher temperatures. In addition, the thermostability was positively related to its molecular weight but also affected by the inherent structures, such as β -O-4 linkages and condensed units. However, as an integrated biorefinery process for XOS, high-purity lignin, and bioethanol, the optimal condition for the integrated process should be balanced along with some other aspects, such as cost, operability, and target product, to achieve overall goals. In short, an enhanced understanding of lignin structure features during the integrated process will be beneficial to value-added applications of abundant lignin fractions in a biorefinery process.

■ AUTHOR INFORMATION

Corresponding Author

*(R.-C.S.) Phone: +86 10 62336903. Fax: +86 10 62336903. E-mail: rcsun3@bjfu.edu.cn.

Funding

We are extremely grateful for financial support from the State Forestry Administration (201204803), Major State Basic Research Projects of China (973-2010CB732204/3, 973-2012CB215302), and 863-project (2012AA023204).

Notes

The authors declare no competing financial interest.

■ REFERENCES

- Ragauskas, A. J.; Beckham, G. T.; Biddy, M. J.; Chandra, R.; Chen, F.; Davis, M. F. et al. Lignin valorization: improving lignin processing in the biorefinery. *Science* **2014**, *344*, DOI: 10.1126/science.1246843.
- Liu, S.; Lu, H.; Hu, R.; Shupe, A.; Lin, L.; Liang, B. A sustainable woody biomass biorefinery. *Biotechnol. Adv.* **2012**, *30*, 785–810.
- Alfani, F.; Gallifruoco, A.; Saporosi, A.; Spera, A.; Cantarella, M. J. Comparison of SHF and SSF processes for the bioconversion of steam-exploded wheat straw. *J. Ind. Microbiol. Biotechnol.* **2000**, *25*, 184–192.
- Liu, C.; van der Heide, E.; Wang, H.; Li, B.; Yu, G.; Mu, X. Alkaline twin-screw extrusion pretreatment for fermentable sugar production. *Biotechnol. Biofuels* **2013**, *6*, 97.
- Ishizawa, C. I.; Davis, M. F.; Schell, D. F.; Johnson, D. K. Porosity and its effect on the digestibility of dilute sulfuric acid pretreated corn stover. *J. Agric. Food Chem.* **2007**, *55*, 2575–2581.

- (6) Karagöz, S.; Bhaskar, T.; Muto, A.; Sakata, Y. Comparative studies of oil compositions produced from sawdust, rice husk, lignin and cellulose by hydrothermal treatment. *Fuel* **2005**, *84*, 875–884.
- (7) Walch, E.; Zemann, A.; Schinner, F.; Bonn, G.; Bobleter, O. Enzymatic saccharification of hemicellulose obtained from hydrothermally pretreated sugar cane bagasse and beech bark. *Bioresour. Technol.* **1992**, *39*, 173–177.
- (8) Cybulski, I.; Lei, H.; Julson, J. Hydrothermal pretreatment and enzymatic hydrolysis of prairie cord grass. *Energy Fuels* **2009**, *24*, 718–727.
- (9) Pronyk, C.; Mazza, G.; Tamaki, Y. Production of carbohydrates, lignins, and minor components from triticale straw by hydrothermal treatment. *J. Agric. Food Chem.* **2011**, *59*, 3788–3796.
- (10) Prakasham, R. S.; Nagaiah, D.; Vinutha, K. S.; Uma, A.; Chiranjeevi, T.; Umakanth, A. V.; et al. Sorghum biomass: a novel renewable carbon source for industrial bioproducts. *Biofuels* **2014**, *5*, 159–174.
- (11) Lu, H.; Hu, R.; Ward, A.; Amidon, T. E.; Liang, B.; Liu, S. Hot-water extraction and its effect on soda pulping of aspen woodchips. *Biomass Bioenergy* **2012**, *39*, 5–13.
- (12) Lu, X.; Zhang, Y.; Angelidaki, I. Optimization of H_2SO_4 -catalyzed hydrothermal pretreatment of rapeseed straw for bioconversion to ethanol: focusing on pretreatment at high solids content. *Bioresour. Technol.* **2009**, *100*, 3048–3053.
- (13) Gould, J. M. Alkaline peroxide delignification of agricultural residues to enhance enzymatic saccharification. *Biotechnol. Bioeng.* **1984**, *26*, 46–52.
- (14) Dang, V. Q.; Nguyen, K. L. A universal kinetic equation for characterising the fractal nature of delignification of lignocellulosic materials. *Cellulose* **2007**, *14*, 153–160.
- (15) Kaparaju, P.; Felby, C. Characterization of lignin during oxidative and hydrothermal pre-treatment processes of wheat straw and corn stover. *Bioresour. Technol.* **2010**, *101*, 3175–3181.
- (16) Doherty, W. O.; Mousavioun, P.; Fellows, C. M. Value-adding to cellulosic ethanol: lignin polymers. *Ind. Crops Prod.* **2011**, *33*, 259–276.
- (17) Zhao, J.; Wilkins, R. M. Controlled release of the herbicide, fluometuron, from matrix granules based on fractionated organosolv lignins. *J. Agric. Food Chem.* **2003**, *51*, 4023–4028.
- (18) Zhang, X.; Tu, M.; Paice, M. G. Routes to potential bioproducts from lignocellulosic biomass lignin and hemicelluloses. *Bioenergy Res.* **2011**, *4*, 246–257.
- (19) Sluiter, A.; Hames, B.; Ruiz, R.; Scarlata, C.; Sluiter, J.; Templeton, D.; Crocker, D. *Determination of Structural Carbohydrates and Lignin in Biomass*; Technical Report NREL/TP-510-42618; National Renewable Energy Laboratory: Golden, CO, USA, 2008.
- (20) Sun, S. L.; Wen, J. L.; Ma, M. G.; Li, M. F.; Sun, R. C. Revealing the structural inhomogeneity of lignins from sweet sorghum stem by successive alkali extractions. *J. Agric. Food Chem.* **2013**, *61*, 4226–4235.
- (21) Granata, A.; Argyropoulos, D. S. 2-Chloro-4,4,5,5-tetramethyl-1,3,2-dioxaphospholane, a reagent for the accurate determination of the uncondensed and condensed phenolic moieties in lignins. *J. Agric. Food Chem.* **1995**, *43*, 1538–1544.
- (22) Wen, J. L.; Sun, S. L.; Yuan, T. Q.; Xu, F.; Sun, R. C. Structural elucidation of lignin polymers of eucalyptus chips during organosolv pretreatment and extended delignification. *J. Agric. Food Chem.* **2013**, *61*, 11067–11075.
- (23) Samuel, R.; Cao, S.; Das, B. K.; Hu, F.; Pu, Y.; Ragauskas, A. J. Investigation of the fate of poplar lignin during autohydrolysis pretreatment to understand the biomass recalcitrance. *RSC Adv.* **2013**, *3*, 5305–5309.
- (24) Sannigrahi, P.; Kim, D.-H.; Jung, S.; Ragauskas, A. Pseudo-lignin and pretreatment chemistry. *Energy Environ. Sci.* **2011**, *4*, 1306–1310.
- (25) Leschinsky, M.; Zuckerstätter, G.; Weber, H. K.; Patt, R.; Sixta, H. Effect of autohydrolysis of Eucalyptus globulus wood on lignin structure. Part 1: comparison of different lignin fractions formed during water prehydrolysis. *Holzforschung* **2008**, *62*, 645–652.
- (26) Wen, J. L.; Xue, B. L.; Xu, F.; Sun, R. C.; Pinkert, A. Unmasking the structural features and property of lignin from bamboo. *Ind. Crops Prod.* **2013**, *42*, 332–343.
- (27) Faix, O. Classification of lignins from different botanical origins by FT-IR spectroscopy. *Holzforschung* **1991**, *45*, 21–28.
- (28) Sun, S. L.; Wen, J. L.; Ma, M. G.; Sun, R. C.; Jones, G. L. Structural features and antioxidant activities of degraded lignins from steam exploded bamboo stem. *Ind. Crops Prod.* **2014**, *56*, 128–136.
- (29) Wen, J. L.; Sun, S. N.; Yuan, T. Q.; Xu, F.; Sun, R. C. Fractionation of bamboo culms by autohydrolysis, organosolv delignification and extended delignification: understanding the fundamental chemistry of the lignin during the integrated process. *Bioresour. Technol.* **2013**, *150*, 278–286.
- (30) Del Río, J. C.; Rencoret, J.; Prinsen, P.; Martínez, A. N. T.; Ralph, J.; Gutiérrez, A. Structural characterization of wheat straw lignin as revealed by analytical pyrolysis, 2D-NMR, and reductive cleavage methods. *J. Agric. Food Chem.* **2012**, *60*, 5922–5935.
- (31) Martínez, Á. T.; Rencoret, J.; Marques, G.; Gutiérrez, A.; Ibarra, D.; Jiménez-Barbero, J.; Del Río, J. C. Monolignol acylation and lignin structure in some nonwoody plants: a 2D NMR study. *Phytochemistry* **2008**, *69*, 2831–2843.
- (32) Ralph, J.; Lundquist, K.; Brunow, G.; Lu, F.; Kim, H.; Schatz, P. F.; et al. Lignins: natural polymers from oxidative coupling of 4-hydroxyphenyl-propanoids. *Phytochem. Rev.* **2004**, *3*, 29–60.
- (33) Sun, S. N.; Cao, X. F.; Xu, F.; Sun, R. C.; Jones, G. L. Structural features and antioxidant activities of lignins from steam exploded bamboo (*Phyllostachys pubescens*). *J. Agric. Food Chem.* **2014**, *62*, 5939–5947.
- (34) Wen, J. L.; Sun, S. L.; Xue, B. L.; Sun, R. C. Recent advances in characterization of lignin polymer by solution-state nuclear magnetic resonance (NMR) methodology. *Materials* **2013**, *6*, 359–391.
- (35) Wen, J. L.; Xue, B. L.; Xu, F.; Sun, R. C. Quantitative structural characterization of the lignins from the stem and pith of bamboo (*Phyllostachys pubescens*). *Holzforschung* **2013**, *67*, 613–627.
- (36) Wen, J. L.; Sun, S. L.; Xue, B. L.; Sun, R. C. Quantitative structures and thermal properties of birch lignins after ionic liquid pretreatment. *J. Agric. Food Chem.* **2013**, *61*, 635–645.
- (37) Sette, M.; Wechselberger, R.; Crestini, C. Elucidation of lignin structure by quantitative 2D NMR. *Chem.–Eur. J.* **2011**, *17*, 9529–9535.
- (38) El Hage, R.; Chrusciel, L.; Desharnais, L.; Brosse, N. Effect of autohydrolysis of *Miscanthus × giganteus* on lignin structure and organosolv delignification. *Bioresour. Technol.* **2010**, *101*, 9321–9329.
- (39) Pu, Y. Q.; Cao, S. L.; Ragauskas, A. Application of quantitative ^{31}P NMR in biomass lignin and biofuel precursors characterization. *J. Energy Environ. Sci.* **2011**, *4*, 3154–3166.
- (40) Crestini, C.; Argyropoulos, D. S. Structural analysis of wheat straw lignin by quantitative ^{31}P and 2D NMR spectroscopy. The occurrence of ester bonds and α -O-4 substructures. *J. Agric. Food Chem.* **1997**, *45*, 1212–1219.
- (41) Hodgson, E.; Nowakowski, D.; Shield, I.; Riche, A.; Bridgwater, A. V.; Clifton-Brown, J. C.; et al. Variation in *Miscanthus* chemical composition and implications for conversion by pyrolysis and thermochemical bio-refining for fuels and chemicals. *Bioresour. Technol.* **2011**, *102*, 3411–3418.
- (42) Sun, R. C.; Tomkinson, J.; Jones, G. J. Fractional characterization of ash-AQ lignin by successive extraction with organic solvents from oil palm EFB fibre. *Polym. Degrad. Stab.* **2000**, *68*, 111–119.
- (43) Raveendran, K.; Ganesh, A.; Khilar, K. C. Influence of mineral matter on biomass pyrolysis characteristics. *Fuel* **1995**, *74*, 1812–1822.